

# Color Change from Black to Green In Chromate Conversion Coatings: A Study by Scanning Electron Microscopy

By I. Song, J.H. Payer, R. Painter and M. Marzano

**The origin of time-dependent color change from black to green in chromate coatings was investigated by using a field-emission-gun scanning electron microscope (FEG-SEM). The distribution of silver, which is known to be responsible for the black appearance of a chromate coating, was examined by back-scattered electron imaging technique. The comparison of back-scattered electron images with secondary electron images clearly contrasted the differences in size and distribution of silver particles between black and green chromate coatings. In a black chromate coating, silver appeared to be distributed finely and uniformly, with a particle size approximately 0.5  $\mu\text{m}$  or less. In contrast, the silver in the coating that had been degraded from black to green appeared as large aggregates on the order of 1  $\mu\text{m}$  or larger. The role of silver in the chromate conversion coating and the accompanying color changes are reviewed. Also discussed is the underlying chemistry, along with well-known physical principles that can lead to the color change from black to green.**

Chromate conversion coating is a widely used method of covering structural components for enhancement of corrosion resistance and the appearance of the components. For aesthetic purposes, the color of the chromate coating is varied. This is done by adjusting the chemistry of the chromating bath and the processes. One of the common colors is black, obtained by adding silver to the chromating bath.<sup>1</sup> The black chromate coating provides a noble appearance, as well as corrosion resistance, to the substrate structure. The combination of corrosion resistance, aesthetic appearance, ease of use and economics has meant wide acceptance of chromate conversion coatings for protecting zinc electrodeposits. Occasionally, however, coating applications engineers have found that, within a few days after the coating process, the black color of the chromate coating changes to green. This unacceptable result has raised serious concern among the engineers and the coating formulation manufacturers.<sup>2,3</sup>

Van de Leest and Wessels<sup>2</sup> presented a summary of their studies of the cause of color changes (black-to-green, black-to-white, etc.), based on analyses of the potential-pH (Pourbaix) diagrams of constituent metals (*i.e.*, silver, chromium and zinc) of black chromate coatings. The approach was an electrochemical interpretation of the stability of insoluble species (metal and passive oxide) in various pH and potential conditions. They concluded that the change of color is the result of corrosion of the silver in the chromate coating and suggested that the black coating can be stabilized by a suitable post-treatment in the rinsewater at a pH of 2 to 6 and a redox potential of about +1 V-NHE.

Generally, it has been assumed that the black color of the chromate coating is caused by fine dispersion of metallic silver particles in the otherwise green chromate coating

matrix, but until now, neither the details of the mechanism of color change nor the chemical state of the coating ingredients has been clearly understood. No report on spectroscopic data is available for the chemical state of silver, and it is uncertain whether silver remains as a metallic phase or forms mixed oxide compounds with other constituents. Moreover, the size, shape and distribution of the silver or silver-containing particles are not understood.<sup>2</sup>

Black is a state in which all wavelengths (at least, all visible wavelengths) are uniformly absorbed by an object, or the waves reflected are completely cancelled. If a certain wavelength (*e.g.*, 515 nm) is preferentially reflected, the human eye will perceive that wave as a green color. Consequently, the color of an object is determined by physical properties of the material—absorbance (A), reflectance (R) and transmittance (T)—where the sum (A + R + T) is essentially unity. The color is also affected by the surface roughness of the object when the roughness becomes comparable to the wavelength of visible light.<sup>4</sup> Under a special condition characterized by Bragg's law, diffraction can occur on such surfaces.<sup>5</sup> An example is the diffraction grating. The diffraction is a reflection resulting from a special condition (Bragg's law). The term, black color, is often used herein to indicate black appearance in the general sense, even though black, by strict definition, is not a color.

The black appearance of an object can be explained via several theories, including free electron theory,<sup>6</sup> Moth's Eye Principle,<sup>7,8</sup> grid theory,<sup>9</sup> and effective medium theory.<sup>10-13</sup> The free electron theory describes the behavior of electrons in solids based on the Drude model. Free electrons absorb photons (*i.e.*, light), make a transition to a higher energy state, then decay (*e.g.*, thermal) back to the lower energy state. An example of free electron theory on the black appearance of an object is the black color of metal oxides (*e.g.*,  $\text{TiO}_2$ ) in reduced, nonstoichiometric states. When an oxide is reduced (*e.g.*,  $\text{TiO}_{2-y}$ ), the charge carrier (*i.e.*, free electron) density increases to maintain the overall charge neutrality. The oxide with an increased number of free electrons will then be able to absorb light effectively over a wide range of the visible spectrum.

Clapham and Hutley have shown that the surface reflection can be controlled by adjusting the size and distribution of the surface feature.<sup>7</sup> This is known as the Moth's Eye Principle. According to this principle, at a certain ratio of thickness,  $d$ , of the surface feature to the wavelength,  $\lambda$ , the reflectance becomes essentially zero. The reported ratio,  $d/\lambda$ , for the minimum reflectance is approximately 0.4. Accordingly, for visible light, the size of the surface feature for the practical minimum of reflectance is estimated to be approximately 0.2  $\mu\text{m}$ .

The grid theory by Ulrich,<sup>9</sup> originally developed for far-infrared filters, describes the optical properties (reflectivity and transmissivity) of thin metallic mesh (inductive) and its complementary (capacitive) grids on a dielectric medium in

the nondiffraction region ( $\lambda > g$ ;  $g$ : grid constant). In his model, the absorption component was estimated to be negligibly small (*i.e.*, it can be considered that  $T + R \sim 1$ ). The result of the transmissivity measurements on the inductive and capacitive grids is in agreement with Clapham and Hutley.<sup>7</sup> Ulrich indicated the possibility of making interference filters consisting of two or more grids of either type. The formation of interference filters may be relevant to the black chromate coating because the coating is considered to consist of metallic silver in a chromium oxide matrix.

Granqvist and Hunderi offered the effective medium theory to explain the optical properties of ultrafine gold particles.<sup>10</sup> Similar examples of this theory have been reported for black coating of various metals and compounds (*e.g.*, Ni, Cr, Mg-Li, MgS, ZnO, with particle size ranging from 0.1 to 1  $\mu\text{m}$ ) for solar energy conversion devices.<sup>14-17</sup> As indicated by the authors, the effective medium theories are mean-field theories (*i.e.*, the nature of the local surrounding of the particles is neglected).

The physical models and theories described above suggest several ways that an object can appear as black. Accordingly, if the black color of the chromate coating results from fine dispersion of metallic silver particles, as suggested by Van de Leest and Wessels,<sup>2</sup> and if one of the theories above can satisfactorily explain the black appearance of the chromate coating, it may be possible to explain the cause of color change from black to green with the aid of electrochemical and physical principles.

In this study, to help identify the cause of color changes from black to green in the chromate coating, the physical state (shape, size, distribution, etc.) of silver in the coating was investigated by using a scanning electron microscope equipped with a field-emission gun (FEG-SEM). The use of the FEG-SEM permitted examination of the coating specimens without forming a conductive layer (*e.g.*, sputter deposition of gold, palladium or carbon) on the specimens. For high resolution studies, often the deposited conductive layer masks the details. Moreover, the element used for the deposition can alter the contrast in the back-scattered electron image and can complicate the elemental analysis of the specimen. Scanning electron microscopy is a useful technique for this study because of the large difference in atomic number between <sup>47</sup>Ag and other constituents (<sup>8</sup>O, <sup>16</sup>S, <sup>24</sup>Cr, and <sup>30</sup>Zn) of the coating. In back-scattered electron images, especially, the large difference in atomic numbers highlights the area of higher silver content in the chromate matrix. Because of this, the results revealed the shape, size and distribution of silver within the chromate coating and contrasted the differences between black and green coating specimens. The morphology of silver precipitates formed on a zinc-plated steel specimen was also determined. The condition was similar to the black chromating bath except that the solution was free of chromium species. The morphology of silver precipitates provided a useful benchmark for the size, shape and distribution of silver in actual black chromate coatings. Based on these physical observations, several possible and probable mechanisms of the process of color change will be discussed.

### Experimental Procedure

Three different specimens were examined: (1) silver, precipitated on a Zn/steel panel (10 x 7 cm), prepared in the lab; (2) black chromate coating that maintained the black color, sampled from the field; and (3) black chromate coating that turned green, sampled from the field. The precipitation of

silver particles on Zn/steel substrate was achieved by immersing a steel sheet (with approximately 180  $\mu\text{m}$  electroplated zinc layer on it) in 4 wt percent  $\text{AgNO}_3$  aqueous solution of pH 1 for 60 sec at room temperature in air, followed by water rinsing and air drying. The field-sampled black and green specimens were originally coated with a commercial formula.<sup>a</sup> The primary ingredients of this formula are  $\text{CrO}_3$  (approximately 20 g/L) and  $\text{AgNO}_3$  (approximately 300 ppm with respect to Ag) with low levels of anions (*e.g.*,  $\text{NO}_3^-$  and  $\text{SO}_4^{2-}$ ). The history of the field-sampled specimens is not known, but it is not considered critically important for the current study because the premise of this work is to identify the difference in physically observable parameters and to discuss the mechanism of the color change based on those observations.

For morphological examinations, a high-resolution (15  $\text{\AA}$  lateral at 15 kV) scanning electron microscope<sup>b</sup> with a field-emission gun was used. In addition to its high resolution, the use of the FEG-SEM was advantageous because sputter deposition of a conductive layer (500-1000  $\text{\AA}$ ) on the specimen, which is often required to prevent the specimen from being electrically charged under the electron beam, is not necessary. This is important for two reasons: (1) the sputter-coated layer will interfere with and/or degrade the back-scattered electron signal, and (2) fine details of the order of the thickness of the conductive layer will become obscure. Secondary electron images were recorded for general examination of surface morphology. Back-scattered electron images were taken for identification of the shape, size and distribution of silver precipitates. Atoms with higher atomic numbers back-scatter more strongly than those with lower atomic numbers. Accordingly, a feature consisting of a higher atomic number appears brighter in the back-scattered electron images.

The back-scattered images were obtained at two different acceleration voltages: 15 kV and 30 kV. This allowed comparison of the back-scattered images and provided information pertaining to the depth-wise distribution of silver in the specimen. In the back-scattered electron imaging mode, sampling depth increases with the acceleration voltage so long as the species of interest is within a depth smaller than the mean free path of the back-scattered electron. Energy dispersive spectroscopy (EDS) measurements were made by using an EDS system<sup>c</sup> attached to the FEG-SEM. The EDS system is equipped with a Si(Li) detector<sup>d</sup> at the specified energy resolution of 143 eV. EDS data were taken at 15 kV acceleration voltage and at 15 mm working distance. The total detector livetime was 200 sec for each spectral data acquisition. Each spectrum consisted of 2048 data points at 10 eV intervals. The data were acquired with the electron beam stopped at features of interest. The electron beam size was less than 30  $\text{\AA}$ .

### Results and Discussion

Figure 1 shows a secondary electron micrograph (15 kV) of silver precipitates formed on zinc-plated steel. The specimen was prepared by immersing a zinc-plated steel sheet in aqueous  $\text{AgNO}_3$  solution (4 wt percent  $\text{AgNO}_3$ , pH 1, room

<sup>a</sup> Pavchrome Black, Pavco Inc., Cleveland, OH.

<sup>b</sup> Model S4500, Hitachi, Japan.

<sup>c</sup> Voyager II, X-ray Quantitative Microanalysis System, Model 2110, Noran Instruments, Middleton, WI.

<sup>d</sup> Model 440B-3SPT, Noran Instruments, Middleton, WI.

<sup>e</sup> Novar, Noran Instruments, Middleton, WI.

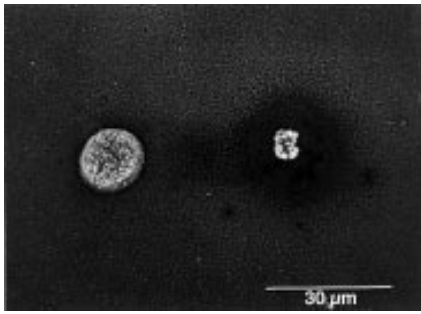


Fig. 1—Electron micrograph (secondary electron image) of Zn/steel surface treated with  $\text{AgNO}_3$ .

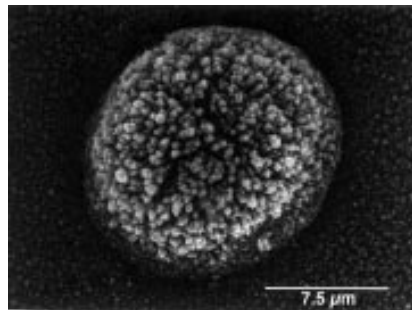


Fig. 2—Electron micrograph (secondary electron image) of Zn/steel surface treated with  $\text{AgNO}_3$ . Higher magnification of the larger of the two large aggregates in Fig. 1.

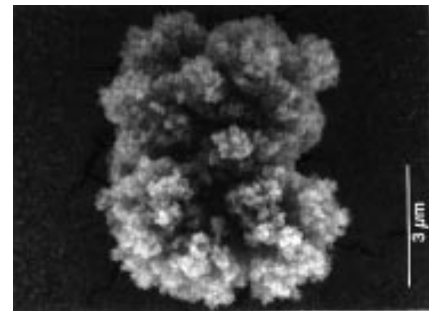


Fig. 3—Electron micrograph (secondary electron image) of Zn/steel surface treated with  $\text{AgNO}_3$ . Higher magnification of the smaller of the two large aggregates in Fig. 1.

temperature, in air, for 60 sec). Two large aggregates consisting of fine precipitates ( $<0.5 \mu\text{m}$ ) can be noted in the background of uniformly distributed small particles. Also, depletion of the small particles around the smaller of the two large aggregates can be seen. This depletion probably occurred when the specimen was being prepared in the aqueous  $\text{AgNO}_3$  solution. Specifically, during the nucleation and growth stage, the exaggerated growth of one particle occurred at the expense of the redissolution of smaller particles. In Fig. 2, the larger of the two large aggregates shown in Fig. 1 is shown at higher magnification. The details of the fine precipitates constituting the large aggregate are clearly observable. Similarly, Fig. 3 offers a more magnified view of the smaller of the two large aggregates shown in Fig. 1.

Figure 4 shows an electron micrograph of a chromate coating specimen that was initially black, but that turned green at some later time. The back-scattered electron image shown on the right half exhibits some variations in contrast, which is believed to be the result of variation of silver content within the chromate coating. Bright spots are clearly noticeable along the edges of the cracks in the back-scattered electron image. It is inferred that these bright spots contain a larger amount of silver than the surroundings because of the reasons to be described below.

Figure 5 shows an electron micrograph of the same chromate coating specimen shown in Fig. 4, but at higher magnification. The back-scattered electron image (right half) clearly shows features ( $\sim 0.25 \mu\text{m}$ ) at the cracked faces. These features are the particles with higher silver content relative to the surroundings. This interpretation is based on (1) the fact that the heavier elements (*i.e.*, higher atomic numbers) appear brighter in the back-scattered image, and (2) the fact that the

difference in atomic number is large between silver and the rest of the coating constituents.

In Fig. 6, for a spectral comparison of the two features at a glance, two EDS spectra (one from a bright feature shown in Fig. 5, and the other from a dark area around the bright feature), that were normalized with respect to the Zn  $K_{\alpha}$  fluorescence X-ray emission line, are shown. Normalization allowed a qualitative comparison of the two spectra. The choice of the Zn  $K_{\alpha}$  line over other strong spectral features for the spectral normalization was because it has sufficient energy to be less subject to absorption by the specimen itself and the EDS detector window material<sup>6</sup>. Also, it has more sufficiently high event counts (approximately 500 counts in the raw data) than other high energy lines (*e.g.*, approximately 100 counts of the Zn  $K_{\alpha}$  line). The EDS data indicate that the feature, which appears bright in the back-scattered image shown in Fig. 5, contains a larger amount of silver than the surroundings. Similar behavior is observed for sulfur and chromium. It is important to point out, however, that interpretation of the low energy features (*e.g.*, carbon  $K_{\alpha}$ , oxygen  $K_{\alpha}$ , chromium  $L_{\alpha}$ , chromium  $L_{\beta}$ , zinc  $L_{\alpha}$ , zinc  $L_{\beta}$ , etc.) requires much more careful analysis, because low-energy X-rays are easily absorbed by the specimen itself, and the results are also affected by the surface morphology (*e.g.*, roughness, etc.). Consequently, analysis of the low-energy features would require serious compensation and correction of the spectra. For the current study, inasmuch as the qualitative comparison of the intensity of silver peaks in the EDS spectra would be sufficient, such corrections were not performed.

In Fig. 7, the back-scattered electron image of the green coating is shown, along with the secondary electron image. In contrast to the micrographs shown in Fig. 4, this image was taken at a higher acceleration voltage (30 kV) to enhance the back-scattered electron contribution of the silver precipitates buried in the coating. Note the blotchy appearance with a few bright spots in the grain from the backscattered image (right half). Also, similar to those shown in Fig. 4, edges around the cracks appear brighter than the inside of the grains. It is observed in Fig. 7 that the size of the particles with higher silver content ranges from 0.5 to 1.5  $\mu\text{m}$ , and that the distance between the particles is greater than 1  $\mu\text{m}$ . For comparison, a secondary electron image and a back-scattered electron image of the black specimen, taken

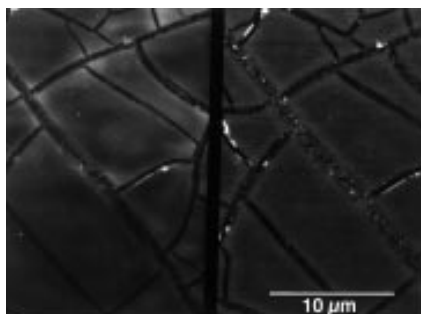


Figure 4—Electron micrograph (secondary and back-scattered electron images) of chromate initially black, but turned green. 15 kV.

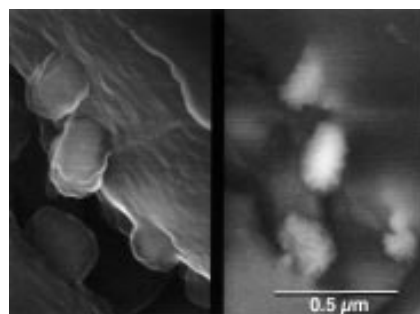


Fig. 5—Electron micrograph (secondary and back-scattered electron images) of chromate coating initially black, but turned green. Higher magnification view of area around a crack shown in Fig. 4. 15 kV.

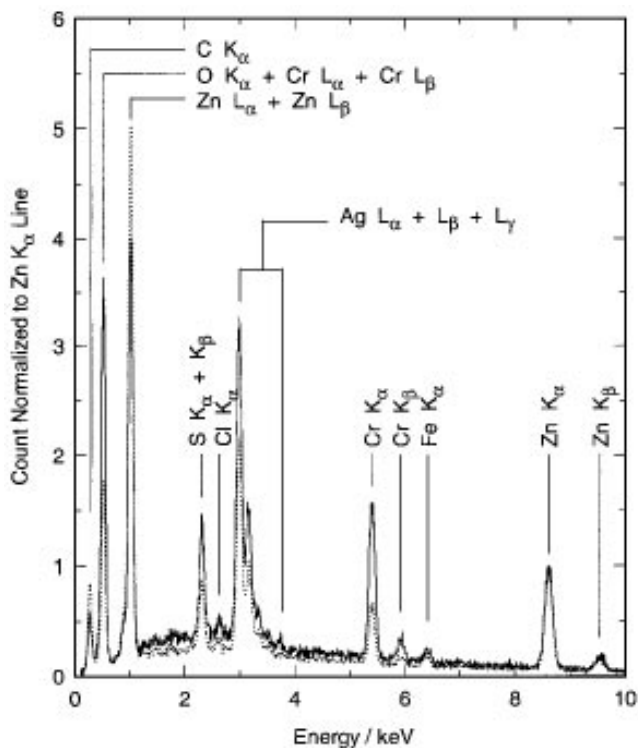


Fig. 6—Energy dispersive spectra of green chromate coating. Solid line represents the bright feature; dotted line depicts the dark area in the back-scattered electron image shown in Fig. 5.

under the same conditions as for Fig. 7 of the green specimen, is shown in Fig. 8. In the back-scattered electron image (right half), note the uniform contrast from cracked edges to the inside of the grains. This indicates that silver-containing particles are uniformly distributed within the chromate coating. Also, note the smaller crack-gap size in the black specimen of Fig. 8 compared to the green specimen shown in Fig. 7. A higher magnification micrograph of the black specimen is shown in Fig. 9 to reveal the details within the crack. In contrast to the green specimen, no significant features were found around the crack faces.

In Fig. 10, a model pathway for the change of color in the chromate coating from black to green is shown. Fine ( $<0.5 \mu\text{m}$ ) silver particles are formed during the coating process, and the particles are uniformly distributed in the coating. This results in a chromate coating with black color, as depicted in Figure 10a. The black coating is characterized by narrow crack width, fine silver particle size and uniform distribution of the silver particles. These characteristics are afforded by

many nucleation sites and a chemical environment suitable for maintaining the stability of the finely dispersed silver particles. By contrast, the green coating is characterized by large crack width, large silver particle size and large spacings between silver particles. Among several ways that the black color of the chromate coating can be changed to other colors, three routes are conceivable for the case of black-to-green color changes: (1) coarsening of metallic silver or compound silver; (2) reaction of fine silver particles with other constituents of the coating to form other compounds or complexes; (3) oxidation/reduction of silver. The first route takes place in a manner similar to Oswald ripening,<sup>17</sup> a well-known mechanism of particle coarsening through solid-state diffusion in many alloy systems. The second route is similar to the mechanism of the coprecipitation process of mixed metal oxide powder from a solution containing the constituents of the mixed oxide powder. The third route is similar to the technique for purification of a material by recrystallization.

For the black-to-green coating conversion, the following process is proposed. During the drying period, a combination of low pH (caused by the drying process) and high oxidizing power (provided by high  $\text{Cr}^{+6}$ ) makes silver unstable, and some silver particles (particularly smaller ones) dissolve into the gelatinous matrix. The dissolved silver will reprecipitate onto existing particles and coalesce to form larger particles near the end of the drying process. During the first few days of the curing period, the chromate coating would be in a gelatinous state and contain some active electrolyte. Under these conditions, the metallic silver particles can be redissolved into the gelatinous electrolytic matrix by the oxidizing action of the residual  $\text{Cr}^{+6}$  in combination with low pH. This situation is depicted in Figure 10b. With further drying of the coating, the dissolved silver ions will precipitate and coalesce to larger metallic aggregates by the reducing action of other oxidizable species, or merely by reprecipitation after reaching the solubility limit toward the end of the drying process. This process is shown in Figure 10c. Consequently, as predicted by the physical theories described earlier, the coating will appear as green (olive drab), which is the default base color of the chromate coating. Concomitant with the change in oxidation state of chromium, the larger crack width observed in the green coating may be attributed to the volume change that occurred in the chromate matrix during the drying process.

At a given  $\text{Cr}^{+6}/\text{Cr}_{\text{total}}$  ratio, it is reasonable to envision that the fine cracks of the black coating are developed by the dehydration of chromium (III, VI) oxides during the drying process, while maintaining the same  $\text{Cr}^{+6}/\text{Cr}_{\text{total}}$  ratio. In the

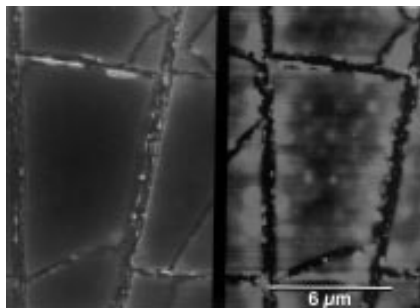


Fig. 7—Electron micrograph (secondary and back-scattered electron images) of chromate coating initially black but turned green. 30 kV.

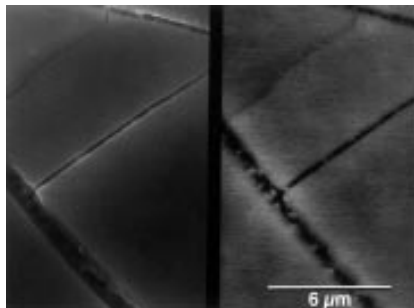


Fig. 8—Electron micrograph (secondary and back-scattered electron images) of chromate coating initially black that remained black. 30 kV, 15 mm working distance.

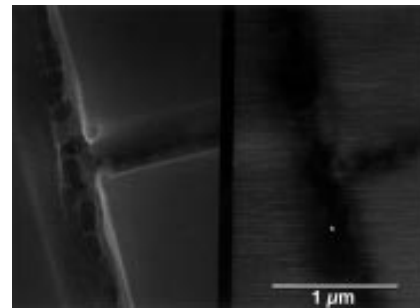


Fig. 9—Electron micrograph (secondary and back-scattered electron images) of chromate coating initially black that remained black. Higher magnification of an area around a crack shown in Fig. 4. 30 kV, 15 mm working distance.

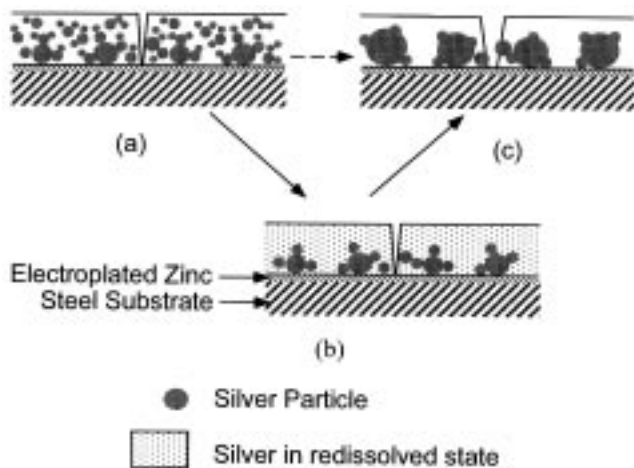


Fig. 10—Model for change of color from black to green: (a) uniform distribution of fine ( $0.5\ \mu\text{m}$ ) silver-containing particles. Black coating characterized by large grain size, narrow crack, fine silver particle size and uniform distribution of silver particles; (b) redissolution of smaller silver particles back to gelatinous chromate coating matrix; (c) coarsening of silver particles by reprecipitation of silver ions dissolved in gelatinous chromate coating matrix at end of drying stage.

case of the green coating, however, it is suspected that more than just the excessive dehydration caused the large crack width. The large cracks of the green coating are created by the change in the structure of the chromium oxide, in addition to the dehydration of the coating, which also occurs in the black chromate coating. The structural change originates from the change in the chemical state of chromium (from VI to III) in the coating, resulting in lowering of the  $\text{Cr}^{+6}/\text{Cr}_{\text{total}}$  ratio. It is worthwhile to note a large difference in the specific volumes of  $\text{CrO}_3$  and  $\text{Cr}_2\text{O}_3$ — $0.37$  and  $0.19\ \text{cm}^3/\text{g}$ , respectively.

As discussed earlier, for a black object, the object appears black for either or both of two main reasons: (1) uniform absorption in all ranges of visible light, (2) uniform cancellation of the amplitude of reflected rays. These suggest that the mechanism of the color change from black to green must be a direct consequence of, or at least closely related to, the changes in the physical state of silver within the chromate coating. The time-dependence of the color change, however, leads to the conclusion that the origin of the color change is in the chemical and/or electrochemical processes that take place within the chromate coating during the curing/drying period. Accordingly, it appears that the color change results from changes in the state (*i.e.*, size and distribution) of silver particles in the chromate coating. This further suggests that an important step to consider is the rinsing/drying/curing process.

The observations of the current study and the relevant theories described above suggest that, in order to have a black appearance, the particle size and distribution should be such that they will cause cancellation of reflected amplitude in all ranges of visible light. In the case of a black chromate coating that turned green, as a result of changes in the size and distribution of silver particles, the default color (olive drab) becomes noticeable. Consequently, it appears that a fine silver particle size ( $<0.5\ \mu\text{m}$ ) and uniform distribution ( $0.1$ – $1\ \mu\text{m}$ ) of the particle within the coating are necessary to maintain the black appearance. For maintaining uniform distribution of fine silver particles, adjustment of the operating parameters (*e.g.*, pH of the rinsewater, length of rinse, temperature of drying air, length of forced drying, etc.) is

recommended during the rinsing and drying period, depending on the production and storage environment (temperature, humidity, etc.).

Black coatings require uniform distribution of fine particles throughout the chromate coating. Failure to form this critical network of particles, or the loss of the critical network by further reaction will result in loss of black appearance. In this paper, without proof, the chemical state of silver has been assumed to be metallic (*i.e.*, elemental). Identification of the chemical state of silver in the chromate coating requires further studies with the aid of spectroscopic techniques. Silver may exist in the metallic state, but it is also possible to exist as the oxide, sulfide, or chloride, and it may even form a complex compound with other constituents of the coating (*e.g.*, Cr, Zn, O, H, etc.).

## Summary

The origin of the color changes from black to green in black chromate coatings was investigated by using a field-emission-gun scanning electron microscope. Use of the FEG-SEM facilitated clear visualization of the distribution of silver particles in the chromate coatings. The secondary electron and back-scattered electron images revealed a major difference in the distribution of silver between a black chromate coating specimen and a black chromate coating specimen that turned green. In the black chromate coating, there was uniform distribution of fine silver particles. By contrast, in the field-returned black chromate coating that turned green, there was irregular distribution of large silver particles.

Observed color changes were rationalized by physical principles, and the relevant chemistry that leads to the color change was discussed. Theories suggest that, to have a black appearance, particle size and distribution should be such that they will cause cancellation of reflected amplitude in all ranges of visible light. In the case of a black chromate coating that turned green, as a result of the changes in the size and distribution of silver particles, the default color (olive drab) becomes noticeable by visual examination. Accordingly, fine silver particle size ( $<0.5\ \mu\text{m}$ ) and uniform distribution ( $0.1$ – $1\ \mu\text{m}$ ) are necessary to maintain the black appearance. To achieve uniform distribution of fine silver particles, it is recommended that adjustment of parameters, such as pH of rinse water, length of rinse, temperature of drying air, length of forced drying, etc., be made during the rinsing and drying period to prevent silver from being redissolved and reprecipitated as larger particles.

The FEG-SEM provided a unique opportunity for direct examination of the morphology and the elemental composition of chromate coatings. The advantage of using the FEG-SEM over a conventional SEM was clearly demonstrated by the ability to image without the use of a conductive coating on the specimen, which can seriously degrade the back-scattered electron signal, can alter the elemental information, and can obscure the fine details of the morphology.

**Editor's note:** Manuscript received, June 1995; revision received, August 1995.

## References

1. H. Geduld, *Zinc Plating*, ASM International, Metals Park, OH, 1988; pp. 139-162.
2. R.E. Van de Leest and J. Wessels, *Plat. and Surf. Fin.*, **67**, 86 (May, 1980).

3. Q.X. Yao, *ibid.*, **75**, 54 (Feb., 1988).
4. R.L. Axelbaum and H. Brandt, *Solar Energy*, **39**, 233 (1987).
5. B.D. Cullity, *Elements of X-ray Diffraction*, 2nd ed., Addison-Wesley, Redding, MA, 1978; pp. 86-87.
6. N.W. Ashcroft and N.D. Mermin, *Solid State Physics*, Holt, Rinehart & Winston, New York, NY, 1976; pp. 16-20.
7. P.B. Clapham and M.C. Hutley, *Nature*, **244**, 281 (1973).
8. B.S. Thornton, *J. Opt. Soc. Am.*, **65**, 267 (1975).
9. R. Ulrich, *Infrared Phys.*, **7**, 37 (1967); *ibid.*, 65.
10. C.G. Granqvist and O. Hunderi, *Phys. Rev.*, **B 16**, 3513 (1977).
11. P. O'Neill and A. Ignatiev, *Phys. Rev.*, **B 18**, 6540-6548.
12. R.B. Stephens and G.D. Cody, *Solar Energy Materials*, **1**, 397 (1979).
13. G. Zajac, G.B. Smith and A. Ignatiev, *J. Appl. Phys.* **51**, 5544 (1980).
14. S.T. Wu and L.W. Masters, *J. Coatings Technol.*, **56**(711), 29-32 (1984).
15. J.S. Vaishya and T.C. Tripathi, *Energy Convers. Mgmt.* **26**, 291 (1986).
16. A. Chandra and M. Mishra, *ibid.*, **28**, 193-195 (1988).
17. A.K. Sharma, R. Uma Rani, H. Bhojaraj and H. Narayanamurthy, *J. Appl. Electrochem.*, **23**, 500 (1993).
18. W.D. Kingery, H.K. Bowen and D.R. Uhlmann, *Introduction to Ceramics*, 2nd ed., John Wiley and Sons, New York, NY 1976; pp. 425-430.



Song



Payer



Painter



Marzano

### About the Authors

Dr. Inho Song is a senior research associate in the Department of Materials Science and Engineering, Case Western Reserve University (CWRU), Cleveland, OH 44106. His interests are in the applications of electrochemical and spectroscopic techniques to the characterization of materials.

Dr. Joe H. Payer is a professor and chairman of the Department of Materials Science and Engineering, CWRU. His research interests are in control of environmental degradation of materials—corrosion, loss of adhesion and wear. He is a Fellow and past president of NACE and a Fellow of ASM.

Richard Painter, CEF, is a technical service engineer with Pavco, Inc., Cleveland, OH. He holds a BS in engineering from Cleveland State University and has 15 years' experience in electroplating.

Mike Marzano is a senior research chemist with Pavco, Inc. His research interests include zinc electroplating additives, conversion coatings and lacquers.